35th Annual International Conference of the IEEE EMBS
Osaka, Japan, 3 - 7 July, 2013

Using an injection signal to reduce motion artifacts in capacitive ECG measurements

Aline Serteyn, Rik Vullings, Mohammed Meftah, Jan Bergmans

Abstract— **Capacitive electrodes are a promising alternative to the conventional adhesive ECG electrodes. They provide more comfort to the patient when integrated in everyday objects (e.g. beds or seats) for long-term monitoring. However, the application of such electrodes is limited by their high sensitivity to motion artifacts. Artifacts caused by variation of the coupling capacitance are studied here. An injection signal is proposed to track these variations in real-time. An adaptive filter then estimates the motion artifact and cancels it from the recorded ECG. The amplitude of the motion artifact is reduced in average by 29 dB in simulation and by 20 dB in a lab environment. Our method has the advantages that it is able to reduce motion artifacts occurring in the frequency band of the ECG and that it does not require knowledge about the measurement system.**

I. INTRODUCTION

Introduced by Richardson in 1967 [1] and developed in the last decade, capacitive electrodes allow biopotential recordings through insulating materials, e.g. clothing. Since no direct skin contact is needed, capacitive electrodes can be integrated in everyday objects, such as beds for long-term unobtrusive monitoring or cars for assisted driving [2]. Recently, capacitive electrodes were evaluated for electrocardiographic (ECG) recordings in clinical settings [3].

Unfortunately, the current capacitive systems are not yet ready to replace the conventional ECG systems. The reason is that capacitive systems suffer from a high sensitivity to various kinds of artifacts often making the recorded ECG signal unreliable.

Three main sources of artifacts were identified: the local triboelectric effect at the body-electrode interface [4], the environmental electromagnetic interferences associated with a poor common-mode rejection ratio of the system [4] and the variation of a charged capacitor due to body motion [5]. The latter artifact source is the focus of this paper. The capacitor formed by the body surface and the electrode is charged by the static charges accumulated on the body and in the sensor. Any variation of this capacitance due to motion creates an artifact in the recorded ECG signal. This artifact is in the frequency band of the ECG ([0.5 120] Hz) and therefore cannot be removed by filtering.

A theoretical model for such an artifact was proposed by Ottenbacher and Heuer in [5]. To remove the artifact, they used an inverse system equation. Their method was validated in simulation [5] and in a lab environment [6]. It works very well but requires exact knowledge of all the model parameters. This knowledge is often not available, limiting the applicability of this approach for artifact removal.

Another method for reducing the artifact due to a varying and charged coupling capacitor was recently tested by Eilbrecht et al. in [7]. They used 3D acceleration signals and manually combined them to estimate the artifact via a classic adaptive filtering scheme. Their method has the limitation that it requires an additional sensor (an accelerometer) that must be synchronized with the capacitive ECG system. Besides, whether or not the accelerometer signal can lead to a good approximation of the artifact has not been studied. Their method is also not yet automated since the selection of which combination of the accelerometer signals leads to the best rejection of artifact is done manually.

To overcome the limitations of the discussed methods, we propose an automated strategy that exploits an injection signal to estimate the motion artifact, and an adaptive filter to subtract this artifact from the recorded signal.

The idea of injecting a known and safe high frequency signal through the skin-electrode interface to estimate impedance changes is not new and has been implemented in many conventional ECG systems, e.g. in [8]. Capacitive ECG systems that make use of signal injection have also been developed recently [9], [10], [11]. However, whether or not an injected signal can effectively serve as a basis for motion artifact reduction in capacitive ECG systems has not been studied so far.

This paper starts with an analysis of the motion artifact based on a model of the capacitive recording system (Section II). Based on the artifact model, we analyse which information the injection signal can provide about the motion artifact (Section III). We use this information as an input to a classic adaptive filtering scheme to estimate the artifact and remove it from the recorded signal (Section IV). A lab experiment is set up to validate our method (Section V). The results of the artifact reduction in simulation as well as on lab data are then presented and discussed (Sections VI and VII).

II. MODEL OF THE CAPACITIVE SYSTEM AND ORIGIN OF THE ARTIFACT

A capacitive sensor measures the displacement current caused by electrical fields on the body surface. Therefore, no galvanic contact to the body is required. The body-electrode interface is represented by a time-varying capacitor $C_c(t)$. The equivalent circuit of a capacitive sensor coupled to a body is shown in Fig. 1 (adapted from [5]). The high input impedance of the capacitive sensor is represented by a bias

A. Serteyn, R. Vullings and J. Bergmans are with the Signal Processing Systems group, Eindhoven University of Technology, The Netherlands. Corresponding author: a.a.m.serteyn@tue.nl

M. Meftah is with the Patient Care Solutions group, Philips Research Eindhoven, The Netherlands

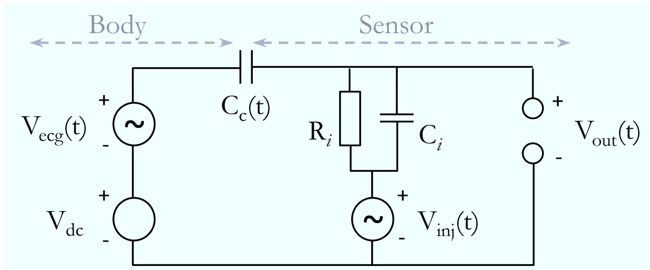

Fig. 1. Equivalent circuit of the capacitive recording system adapted from [5]. The static voltage $V_{\rm dc}$ and the time variations of the coupling capacitor $C_c(t)$ cause an artifact in $V_{\rm out}$. A high-frequency voltage $V_{\rm inj}$ is applied from the electrode side.

resistance R_i in parallel to a capacitor C_i, both assumed to be time invariant. The voltage $V_{\rm ecg}(t)$ stands for the biopotential to be recorded, in this case the ECG. The voltage $V_{\rm inj}(t)$ represents a known sinusoidal injection signal used to gauge the motion artifact. The voltage $V_{\rm dc}$ models the accumulation of static charges on the body surface relative to the capacitive sensor and is here assumed to be time invariant. Finally, $V_{\rm out}(t)$ is the voltage recorded at the output of the measurement system.

The time domain behavior of the capacitive recording system can be described by the differential equation:

$$(C_i + C_c)\frac{\mathrm{d}V_{\rm out}}{\mathrm{d}t} + \Big(\frac{1}{R_i} + \frac{\mathrm{d}C_c}{\mathrm{d}t}\Big)V_{\rm out} = \frac{V_{\rm inj}}{R_i} + C_i\frac{\mathrm{d}V_{\rm inj}}{\mathrm{d}t} + \frac{\mathrm{d}C_cV_{\rm ecg}}{\mathrm{d}t} + \frac{\mathrm{d}C_cV_{\rm dc}}{\mathrm{d}t} \ .$$

This mathematical description of a capacitive recording system was implemented in Simulink (The MathWorks, Inc.) to simulate the system's behavior for different conditions. We also solved the differential equation to gain more insight into the system's behavior. In the simplifying case where $V_{\rm inj} = 0$ and with the initial condition being $V_{\rm out}(t_0) = 0$ or $t_0 = -\infty$, we find that [12]:

$$V_{\rm out}(t) = s(t) + a(t) \tag{1}$$

where

$$s(t) = \frac{1}{C_i+C_c(t)}\int_{t_0}^{t}\frac{\mathrm{d}(C_cV_{\rm ecg})}{\mathrm{d}u}\ h(t,u)\ \mathrm{d}u \tag{2}$$

$$a(t) = \frac{V_{\rm dc}}{C_i+C_c(t)}\int_{t_0}^{t}\frac{\mathrm{d}C_c}{\mathrm{d}u}\ h(t,u)\ \mathrm{d}u \tag{3}$$

and

$$h(t,u) = \mathrm{e}^{-\frac{1}{R_i}\int_u^t \frac{1}{C_i+C_c(s)}\mathrm{d}s} \ .$$

The first term on the right hand side of Eq. 1, $s(t)$, shows that the signal of interest $V_{\rm ecg}(t)$ is filtered by the system and that the filter varies dynamically with $C_c(t)$, introducing a distortion of $V_{\rm ecg}(t)$. The second term on the right hand side of Eq. 1, $a(t)$, represents an unwanted additive artifact in the recorded signal $V_{\rm out}$, linearly proportional to $V_{\rm dc}$. A Simulink simulation of this additive artifact and of the $V_{\rm ecg}$ distortions is given in Fig. 2. These signals were obtained

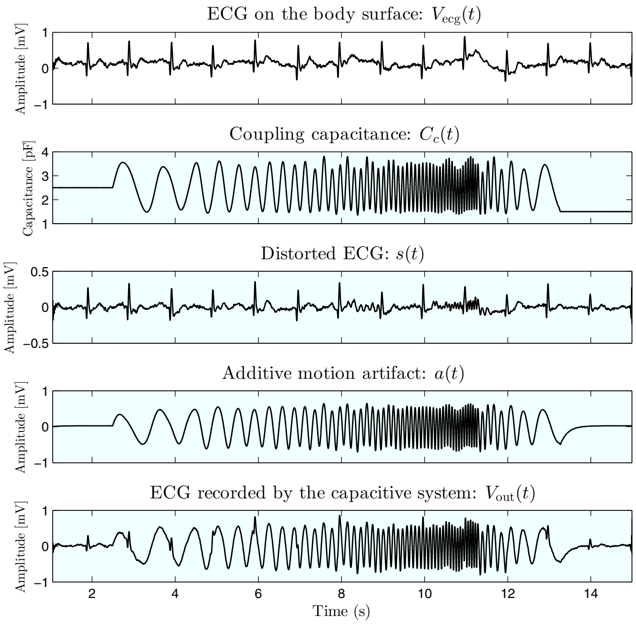

Fig. 2. Illustration of an ECG distortion and a motion artifact present in the recorded ECG. Variations of the coupling capacitance C_c cause, on the one hand, a distortion of the ECG and, on the other hand, an additive artifact in the recorded ECG (see Eq. 1). Graphs from top to bottom: the original ECG signal on the body surface; the variations of C_c between 1.5 and 3.5 pF; the resulting distorted ECG obtained in simulation with $V_{\rm dc} = 0$; the resulting additive artifact obtained in simulation with $V_{\rm ecg} = 0$; the recorded ECG that is the sum of both the distorted ECG and the additive artifact.

with $V_{\rm inj} = 0$, $R_i = 42$ GOhm, $C_i = 2.8$ pF and $C_c \in [1.5\ 3.5]$ pF, these values being representative of our physical capacitive sensor. The coupling capacitance $C_c(t)$ varies at a frequency ranging from 0 to 20 Hz (second graph of Fig. 2). This frequency band was chosen in order to cover motion artifacts due to breathing (0.1-2 Hz) and body movements (0-10 Hz), but also due to ballistocardiograhic vibrations (0-20 Hz) [9]. In these conditions, taking $V_{\rm dc} = 3$ mV leads to an artifact that has an amplitude of about three times that of the recorded ECG (fifth graph of Fig 2). In lab recordings, $V_{\rm dc}$ typically has values of a few millivolts to several volts.

As can be seen in the fifth graph of Fig. 2, the contribution of $a(t)$ in $V_{\rm out}$ poses a much larger problem than the distortion in $s(t)$. We therefore do not further address the ECG distortion here but we focus on suppressing the additive artifact $a(t)$. This can be done in three ways:

- Making C_c time invariant: this requires one to tightly fix the electrodes against the body, reducing comfort and preventing in-object integration.
- Reducing $V_{\rm dc}$: this could be done by a careful implementation of a feedback control loop in the hardware. Since this solution cancels the artifact directly at the source, it is expected to work the best. However, it requires a more complex design of the capacitive sensor.
- Estimating the artifact $a(t)$ and then subtracting it from $V_{\rm out}$: this is the strategy considered here for its simplicity and as a preliminary study.

III. Injection signal and its relation with the artifact

We know from Eq. 3 that the motion artifact $a(t)$ in $V_{\text{out}}(t)$ is a dynamically filtered version of $\frac{\mathrm{d}C_c}{\mathrm{d}t}$. Since V_{dc}, C_c, C_i and R_i are not exactly known in practice, we cannot directly compute and compensate for the artifact. Hence, we injected a known sinusoidal signal $V_{\text{inj}}(t)$ of 50 mV amplitude through the system to track $\frac{\mathrm{d}C_c}{\mathrm{d}t}$.

When $V_{\text{inj}}(t)$ is applied from the electrode side as in Fig. 1, the transfer function of the system is given by:

$$H(j\omega) = \frac{V_{\text{out}}}{V_{\text{inj}}} = \frac{1 + C_i R_i j\omega}{1 + (C_c + C_i) R_i j\omega} \tag{4}$$

At high frequencies, this transfer function becomes a constant gain $H = \frac{C_i}{C_i + C_c}$. In this case and if C_c is time-varying, any variation of $C_c(t)$ will instantaneously affect the contribution of $V_{\text{inj}}(t)$ in the recorded signal $V_{\text{out}}(t)$ via the time-varying gain $H(t)$. In other words, knowing $H(t)$ provides us with direct information about $\frac{\mathrm{d}C_c}{\mathrm{d}t}$. In our case, the gain $H(t)$ is known because it can be obtained directly by demodulating $V_{\text{out}}(t)$ at the frequency of $V_{\text{inj}}(t)$. A frequency of 1 kHz is chosen to be well above the cut-off frequency of $H(j\omega)$. The following relation expresses the link between the variation of $C_c(t)$ and the transfer function for $V_{\text{inj}}(t)$ at high frequencies:

$$\frac{\mathrm{d}C_c}{\mathrm{d}t} = \frac{C_i}{H^2} \frac{\mathrm{d}H}{\mathrm{d}t} \tag{5}$$

where the constant C_i is unknown. From Eq. 3, we know that the artifact $a(t)$ is a dynamically filtered version of $\frac{\mathrm{d}C_c}{\mathrm{d}t}$. Therefore and from Eq. 5, we know that the artifact is a dynamically filtered version of

$$R(t) = \frac{1}{H^2} \frac{\mathrm{d}H}{\mathrm{d}t} \ .$$

IV. Artifact estimation and cancellation

The amplitude gain $H(t)$ of the injection voltage provides us with information about $\frac{\mathrm{d}C_c}{\mathrm{d}t}$ (Eq. 5) and therefore about the artifact $a(t)$ (Eq. 3). Assuming that $H(t)$ and therefore $R(t)$ are uncorrelated with the biopotential V_{ecg}, we propose the artifact cancellation scheme represented in Fig. 3. The filters F1 and F2 depend on C_i, R_i and C_c and are therefore unknown. The signal $R(t)$ is filtered by the adaptive FIR filter in order to approximate the artifact $a(t)$ as well as possible. If $a(t)$ is uncorrelated with $s(t)$, the best artifact approximation $\hat{a}(t)$ is achieved when the energy of the error signal $e(t) = s(t) + a(t) - \hat{a}(t)$ is minimal. Therefore, the coefficients W of the filter are adapted such that they minimize the mean square error $E[e^2(t)] = E[(s(t) + a(t) - W(t)R(t))^2]$. A normalized least mean square (NLMS) algorithm is used to solve this optimization problem. The filter coefficients are thus adapted as $W(t+1) = W(t) - \mu(t)\Delta E[e^2(t)]$ where μ is the step size and Δ the gradient. With the signals being sampled at 8 kHz, the time-varying step size of the adaptive filter was set to $\mu(t) = \max(\frac{1\times10^{-6}}{P(t)}, 4\times10^{-5})$, where $P(t)$ is the average power of $R(t)$ over the filter length, i.e. 0.5 s.

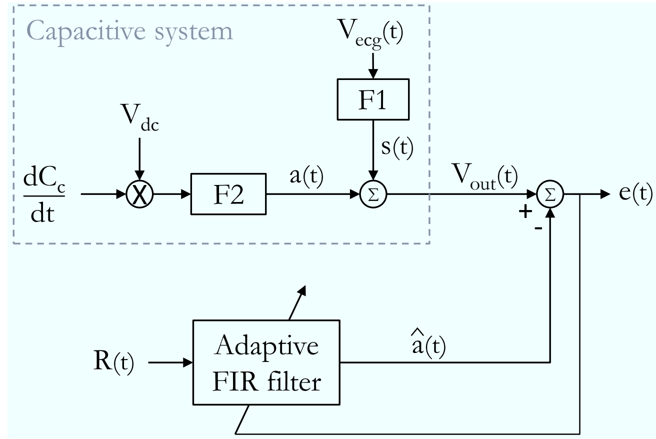

Fig. 3. Artifact cancellation scheme. The coefficients of the FIR filter are adapted (via a NLMS algorithm) such that the energy in the error signal $e(t)$ is minimized. The reference signal $R(t)$ for the adaptive filter is produced via the injection signal (see Section III).

V. Lab data acquisition

To validate our method in a realistic situation, a lab experiment was set up as illustrated in Fig. 4. A shaker connected to a metal plate and controlled by a wave generator was used to simulate the body and body motion. An ECG signal was applied on the metal plate while the plate motion was controlled by sinusoidal and step waves.

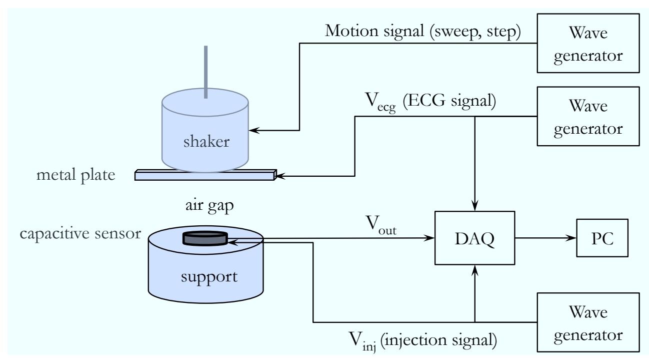

Fig. 4. Lab data acquisition setup. The metal plate and the shaker represent the body surface and the body motion. The metal plate is coupled to the capacitive sensor via an air gap. An injection signal V_{inj} is used to track the distance variations between the metal plate and the capacitive sensor.

VI. Results

A. On simulated data

An illustration of artifact cancellation on simulated data is given in Fig. 5. A first important result is that the estimated motion artifact $\hat{a}(t)$ (second graph) correlates well with the additive artifact observed in V_{out} (first graph). Based on this estimation, the adaptive filter provides a more readable version of V_{out}, as shown in the third graph.

In simulation, the exact artifact $a(t)$ to be estimated and removed from V_{out} is known and the estimation error $a(t) - \hat{a}(t)$ can be computed. The mean estimation error was 0.046 mV for an original artifact of 1.2 mV peak to peak. Therefore, the artifact amplitude was reduced to 3.2% of its initial value, that is a reduction of 29 dB. The remaining

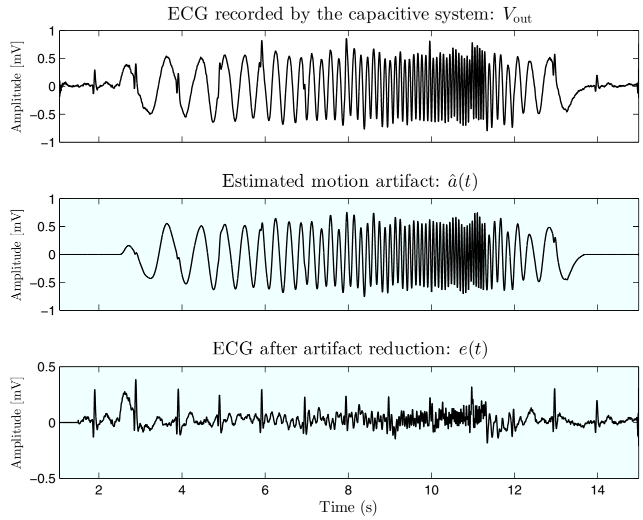

Fig. 5. Artifact cancellation on simulated data. An injection signal and an adaptive filter are used to estimate the artifact $a(t)$ (2nd graph) that is subtracted from V_{out} (1st graph) to obtain the ECG in the third graph.

artifact is on average 10 times smaller than the amplitude of the recorded ECG (0.4 mV).

B. On lab data

The distance between the electrode and the metal plate varied between 2 and 2.5 mm for an electrode area of 2 cm^2. The voltage V_{dc} was about 20 mV and the amplitude of the R-peak in V_{ecg} was 1.3 mV. This led to an artifact that was about four times the amplitude of the recorded ECG. A frequency sweep motion between 0.1 and 25 Hz was applied to the metal plate. The results of the artifact cancellation are shown in Fig. 6. The remaining artifact has approximately 10% of its original value (-20 dB) and is on average three times smaller than the recorded ECG.

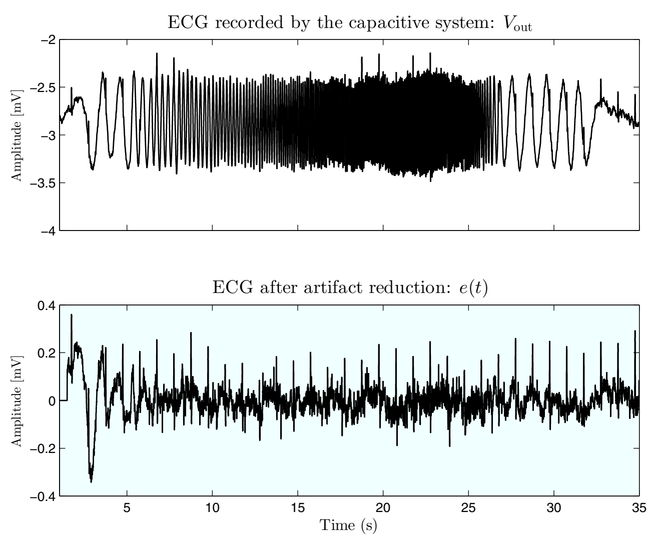

Fig. 6. Artifact cancellation on lab data. The estimated motion artifact is subtracted from V_{out} (1st graph) to obtain the ECG in the second graph.

VII. Conclusion and Future Work

We have shown that significant motion artifact reduction in capacitive electrodes can be achieved by using an injection current combined with an adaptive filter. The greatest advantages of our method are that no auxiliary sensor is needed and that the parameters C_i and R_i do not need to be known or manually tuned. Limitations are that the signal distortion is not corrected and that some residual additive artifacts remain. Our strategy is also based on several assumptions such as a constant V_{dc} and an air gap as body-electrode interface, which avoids triboelectric effects.

Our recommendation for future work is to analyse how Eq. 3 can be better approximated. Using a-priori knowledge about the adaptive filter would permit us to simplify its expression. This would not only allow an easier implementation of the filter for online processing but may also provide a better reduction of the artifact. Future work should also focus on studying the behavior of the adaptive filter as a function of the amplitude of the artifact. Finally, considering a time varying voltage V_{dc} and filling the air gap with textile layers will provide a useful next step towards realistic on-body measurements.

References

[1] P. Richardson, "The insulated electrode: A pasteless electrocardiographic technique," in *20th Ann. Conf. on Engineering in Medicine and Biology*, vol. 15.7, 1967.

[2] J. Schneider, C. Koellner, and S. Heuer, "An approach to automotive ECG measurement validation using a car-integrated test framework," in *Intelligent Vehicles Symposium, 2012 IEEE*, 2012, pp. 950 –955.

[3] M. Czaplik, B. Eilebrecht, R. Walocha, M. Walter, P. Schauerte, S. Leonhardt, and R. Rossaint, "The reliability and accuracy of a noncontact electrocardiograph system for screening purposes," *Anesthesia and Analgesia*, vol. 114, no. 2, pp. 322–327, 2012.

[4] T. Wartzek, T. Lammersen, B. Eilebrecht, M. Walter, and S. Leonhardt, "Triboelectricity in capacitive biopotential measurements," *Biomedical Engineering, IEEE Transactions on*, vol. PP, no. 99, p. 1, 2010.

[5] J. Ottenbacher and S. Heuer, "Motion artefacts in capacitively coupled ECG electrodes," in *World Congress on Medical Physics and Biomedical Engineering, 2009*, ser. IFMBE Proceedings. Springer Berlin Heidelberg, 2010, vol. 25/4, pp. 1059–1062.

[6] S. Heuer, D. Martinez, S. Fuhrhop, and J. Ottenbacher, "Motion artefact correction for capacitive ECG measurement," in *Biomedical Circuits and Systems Conference. IEEE*, 2009, pp. 113 –116.

[7] B. Eilebrecht, T. Wartzek, J. Willkomm, A. Schommartz, M. Walter, and S. Leonhardt, "Motion artifact removal from capacitive ecg measurements by means of adaptive filtering," in *5th European Conference of the International Federation for Medical and Biological Engineering*, ser. IFMBE Proceedings, k. Jobbgy, Ed. Springer Berlin Heidelberg, 2012, vol. 37, pp. 902–905.

[8] D. Buxi, S. Kim, N. Van Helleputte, M. Altini, J. Wijsman, R. Yazicioglu, J. Penders, and C. Van Hoof, "Correlation between electrode-tissue impedance and motion artifact in biopotential recordings," *Sensors Journal, IEEE*, vol. 12, no. 12, pp. 3373 –3383, 2012.

[9] P. Luna-Lozano and R. Pallas-Areny, "Microphonics in biopotential measurements with capacitive electrodes," in *IEEE EMBC*, 2010, pp. 3487 –3490.

[10] T. Wartzek, H. Weber, M. Walter, B. Eilebrecht, and S. Leonhardt, "Automatic electrode selection in unobtrusive capacitive ecg measurements," in *IEEE CBMS*, 2012, pp. 1–4.

[11] K. Mueller, B. Blankertz, G. Curio, and M. Schilling, "Sensor system and methods for the capacitive measurement of electromagnetic signals having a biological origin," US Patent 8 193 821, 2012.

[12] T. Apostol, *Calculus, vol. 1: One-variable calculus with an introduction to linear algebra*. Wiley New York, 1967.